A computing model of ion energy distributions for dual frequencies capacitive couple discharges

Zhuwen Zhou[1,2,3]·, Bo Kong[1,3], Deliang Chen[1,2], Yuee Luo[1,3], and Yuansheng Wang[1,2]

[1]Physics and Electronic Science College, Guizhou Education University, Guiyang 550018, China

[2]Key Laboratory of Photoelectron Materials Design and Simulation in Guizhou Province, Guiyang 550018, China

[3]Scientific Research Innovation Team in Plasma and Functional Thin Film Materials in Guizhou Province, Guiyang 550018, China

E-mail: zzwwdxy@gznc.edu.cn

Abstract. We have developed an analytical dual-frequency model, which results in accurate dual-peaks of the ion energy distributions (IEDs) for the given control parameters. The model can analytically calculate and predict the IEDs dual peaks and energy width with necessary plasma parameters. This model can also predict the IEDs from dual frequencies' drives at any voltage, the associated results are compared with particle-in-cell (PIC) simulations. The IED at a surface is an important parameter for processing in dual radio frequencies driven capacitive couple discharges. The computing model is developed for the IED in a low pressure discharge based on a linear transfer function that relates the time-varying sheath voltage to the time-varying ion energy response at the surface. This model is in good agreement with PIC simulations over a wide range of dual frequencies driven capacitive couple discharge excitations.

1. Introduction

Capacitive radio frequency discharges are widely used for thin film deposition processing of silicon and surface modification in the microelectronics industry. The ion energy distribution (IED) at the substrate surface is an important parameter in these processes. Since the IED is essentially determined by the sheath response, it is necessary to establish the relationship between the control parameters and the sheath response. It is valuable to develop an analytical model and particle in cell (PIC) simulations to better understand the physics of the discharge and more accurately predict the IED. Multiple frequency drives are often used to control the width and the average of the IED. The physics of IEDs in low pressure single frequency capacitive discharges is fairly well understood.[1–3] In some approaches,[4–7] simulations regarding dual frequency ion energy distribution study sheath parameters and conclude that it is possible to control the IED by varying the voltage of the low frequency drive. In another approach,[8] an effective frequency concept has been introduced for dual

· To whom any correspondence should be addressed.

frequency capacitive discharges to determine the width and average of the IED. The effective frequency takes the place of both frequencies and is dependent on the frequencies and voltages of the dual frequency drive. The IED can then be determined as for a single frequency discharge. Dual frequency discharges have drawn much attention due to their independent control of the ion fluxes and ion bombarding energies at the substrates. Semianalytical [9,10] models were developed to understand the mechanics in multi-frequency capacitive discharges to some extent. For both single- and dual-frequencies, research has been performed by experiments [11] and PIC simulations.[5] Analytical collisional sheath models with charge exchange collisions were developed.[12,13] A global model for capacitive discharges in the collisionless sheath model was proposed to understand bimodal for IED of single frequency capacitive discharge.[14] However, understanding the mechanics of multiple frequencies driven discharges is less than adequate. We have developed an analytical multi-frequency model, which results in accurate multi-peaks IEDs for the given control parameters. Incorporating Benoit-Cattin's model [2] our model can analytically predict the IEDs from multi-frequency drives at any voltage with necessary plasma parameters. PIC simulations are used to verify this model.

2. Theory analysis

Benoit-Cattin and Bernard2 analytically calculated the IEDs and DEi for single frequency drive, in the high frequency regime for a collisionless rf sheath, they assumed (i) a constant sheath width, (ii) a uniform sheath electric field, (iii) a sinusoidal sheath voltage, (iv) zero initial ion velocity at the plasma sheath boundary. For the high frequency regime, the ions take many rf cycles to cross the sheath and can no longer respond to the instantaneous sheath voltage. Instead, the ions respond only to an average sheath voltage and the phase of the cycle in which they enter the sheath becomes unimportant, resulting in a narrower IED. In this high-frequency regime, ΔE_i was calculated analytically for a collisionless sheath by Benoit- Cattin et al and found to be directly proportional to $\widetilde{V}_s$、$\overline{V}_s$, and inverse proportional to ω_{hf}. Thus, as ω_{hf} increases, the IED width shrinks and the two peaks of the IED approach each other until, at some point, they can no longer be resolved (see figure 1). Therefore the expressions for the ion energy distributions function (IEDF- f (E)), and ΔE_{hf} at high- frequency are:

$$f(E) = \frac{2n_t}{\omega_{hf}\Delta E_{hf}}[1 - \frac{4}{(\Delta E_{hf})^2}(E - e\overline{V}_s)^2]^{-1/2} \qquad (1)$$

$$\Delta E_{hf} = \frac{2e\widetilde{V}_s}{\omega_{hf}\overline{s}_{hf}}(\frac{2e\overline{V}_s}{M})^{1/2} \qquad (2)$$

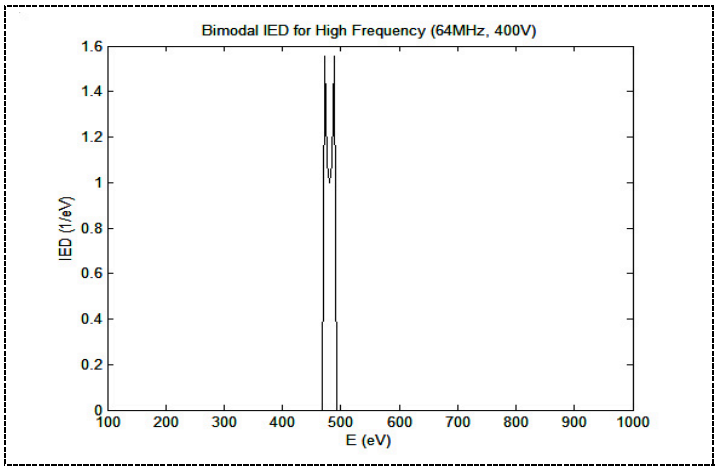

Figure 1. Bimodal IED high frequency (64MHz, 400V).

For the low-frequency regime, the ions cross the sheath in a small fraction of an rf cycle and respond to the instantaneous sheath voltage. Thus, their final energies depend strongly on the phase of the rf cycle in which they enter the sheath. As a result, the IED is broad and bimodal,
and the IED width ΔE_i approaches the maximum sheath drop. The two peaks in the distribution correspond to the minimum and maximum sheath drops (see figure 2). The resulting expressions for f (E) and the ΔE_{lf} at low frequency are

$$f(E) = \frac{2n_t}{\omega_{lf}\Delta E_{lf}}[1 - \frac{4}{(\Delta E_{lf})^2}(E - e\overline{V}_s)^2]^{-1/2} \quad (3)$$

$$\Delta E_{lf} = \frac{2e\widetilde{V}_s}{\omega_{lf}\overline{s}_{lf}}(\frac{2e\overline{V}_s}{M})^{1/2} \quad (4)$$

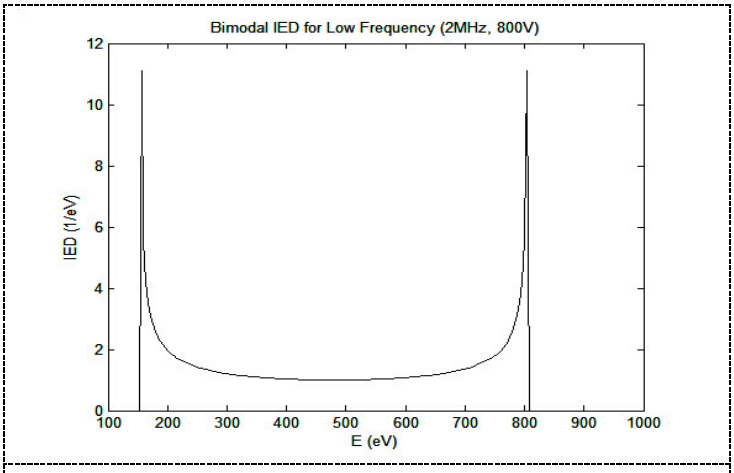

Figure 2. Bimodal IED low frequency (2MHz, 800V).

For the dual-frequency(both high and low frequency) regime, according to Benoit-cattin et al assumed a sinusoidal sheath voltage $V_s(t) = \overline{V}_s + \widetilde{V}_s \sin \omega t$, the sheath voltage functions at dual frequency (2MHz800V, 64MHz400V) showed in Figure 3, dual frequency (3MHz800V, 64MHz400V) showed in figure 4, these figures showed that low frequency voltage of the sheath was modulated by high frequency voltages, so the IED of low frequency sheath voltage was respectively modulated by of high frequency sheath voltage.

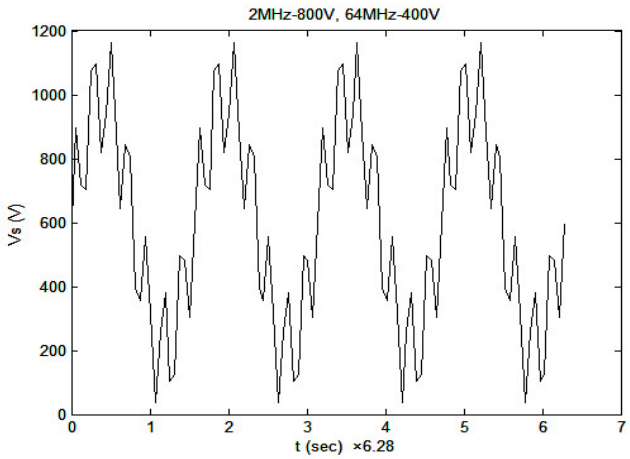

Figure 3. the sheath voltage functions at dual frequency (2MHz800V, 64MHz400V), low frequency (2MHz) voltage of the sheath was modulated by high frequency (64MHz) voltages.

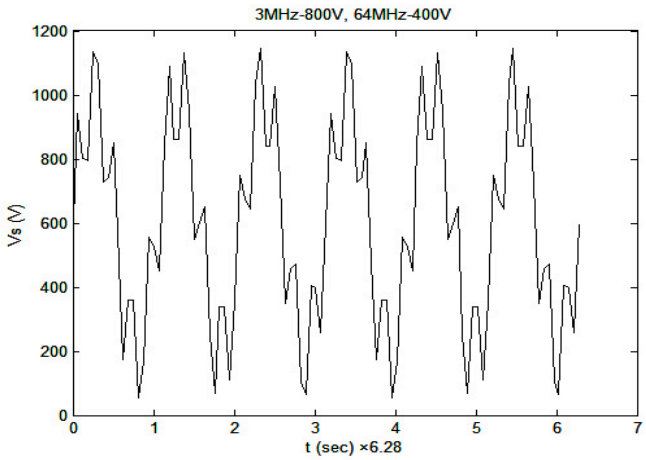

Figure 4. the sheath voltage functions at dual frequency (3MHz800V, 64MHz400V), low frequency (3MHz) voltage of the sheath was modulated by high frequency (64MHz) voltages.

From Eq. (4) we can see, for low frequency regime, the IED width ΔE_i is the max when sheath voltage approaches maximum of peak value, $\Delta E_i = \Delta E_{\max}$, and the bimodal of the IED max width $\Delta E_{\max}$ is in accord with upper and lower limit of IED. More peaks are distributed between the upper and lower limit due to high frequency IED width is small (see Eq. (2)), and its bimodal is repeatedly distributed on the low frequency most width bimodal. We obtain the expressions for the IED, $f(E)$ and the energy width ΔE_{lf}, for dual-frequency regime are:

$$f(E) = \frac{2n_t}{\omega_{lf}\Delta E_{lf}}[1-(\frac{2}{\Delta E_{lf}}(E-e\overline{V}_s))^2]^{-1/2} + \frac{2n_t}{\omega_{hf}\Delta E_{hf}}[1-\frac{4}{(\Delta E_{hf})^2}\sum_n(E-(e\overline{V}_s \pm n\Delta E_{hf}))^2]^{-1/2}$$

$$\Delta E_{lf} = \frac{2e\,\widetilde{V}_s}{\omega_{lf}\bar{s}_{lf}}\left(\frac{2e\overline{V}_s}{M}\right)^{1/2},\ \Delta E_{hf} = \frac{2e\,\widetilde{V}_s}{\omega_{hf}\bar{s}_{hf}}\left(\frac{2e\overline{V}_s}{M}\right)^{1/2}. \tag{5}$$

Where ω_{lf} is low radian frequency of dual-frequency, $\omega_{hf}(>\omega_{lf})$ is higher radian frequency than ω_{lf}. ΔE_{lf} is the most width ion energy distribution relevant to low frequency, the width centre is at $e\overline{V}_s$ with upper limit $e\overline{V}_s + \Delta E_{lf}/2$ and lower limit $e\overline{V}_s - \Delta E_{lf}/2$. ΔE_{hf} is small width ion energy distribution relevant to high frequency, it distribute between upper limit and lower limit of IED. *n* represents integer ratio of $n = \Delta E_{lf}/\Delta E_{hf}$. n_t is the number of ions entering the sheath per unit time. $\bar{s}$ is the average sheath width, and $\overline{V}_s$ is the average sheath potential. We obtain the mean sheath width $\bar{s}$ in terms of the mean sheath voltage $\overline{V}_s$ by using the collisionless Child–Langmuir law

$$\bar{s} = \frac{2}{3}\left(\frac{2e}{M}\right)^{1/4}\left(\frac{\varepsilon_0}{\bar{J}_i}\right)^{1/2}\overline{V}_s^{3/4} \tag{6}$$

The ion current density in the sheath is given by

$$\bar{J}_i = en_s u_B \approx 0.61 n_0 u_B \tag{7}$$

Where n_0 is the bulk plasma density, n_s is the ion density at the pre–sheath boundary and $u_B = (kT_e/M)^{1/2}$ is the Bohm velocity. This implies [1]

$$\bar{s} \approx \frac{2}{3}\left(\frac{2e}{kT_e}\right)^{1/4}\left(\frac{\varepsilon_0}{0.61 n_0 e}\right)^{1/2}\overline{V}_s^{3/4} \tag{8}$$

As the voltage drop across the bulk plasma is relatively small at low pressures, we let, $\widetilde{V}_{rf}$ is the fundamental rf voltage amplitude applied to the electrodes. The time-averaged sheath voltage $\overline{V}_s$, which is also the ion kinetic energy per ion hitting the electrode, ε_i is given by,[3]

$$\varepsilon_i = \overline{V}_s = \widetilde{V}_s/2 \approx 0.8\widetilde{V}_{rf}/2 \tag{9}$$

We illustrated the multi-peaks of IEDs for multi-frequency using the computational analytical model from Eq. (5), (6), (7), (8), (9), for dual frequency excitation with （$\omega_{lf} = 2\pi \times 2$ MHz, $\widetilde{V}_{rf} = 800$ V，$\omega_{hf} = 2\pi \times 64$ MHz, $\widetilde{V}_{rf} = 400$ V, $\bar{s} = 0.0113$ m ） in figure 5, and with（$\omega_{lf} = 2\pi \times 3$ MHz, $\widetilde{V}_{rf} = 800$ V，$\omega_{hf} = 2\pi \times 64$ MHz, $\widetilde{V}_{rf} = 400$ V, $\bar{s} = 0.0113$ m）in figure 6. In order to the model is more truthful, parameter 0.6 instead of 0.8 in Eq. (9). We also compared the model with semi-analytical [10], the IEDs peaks for the model are in accord with semi-analytical.

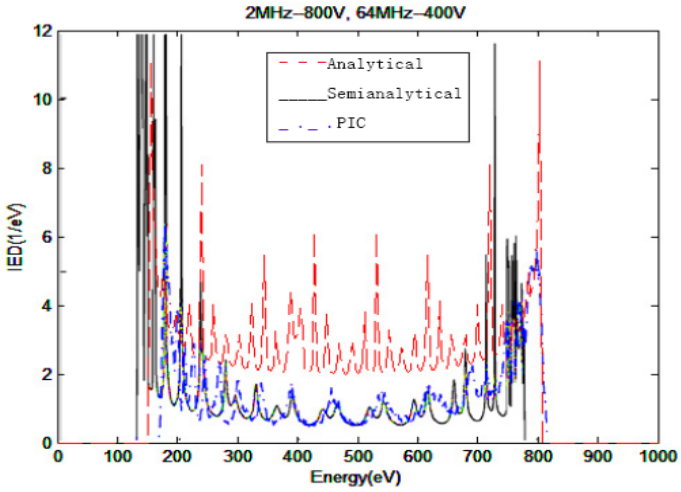

Figure 5.（Color online）Analytical, semianalytical, and PIC IEDs for dual frequency 2MHz - 800V, 64MHz - 400V.

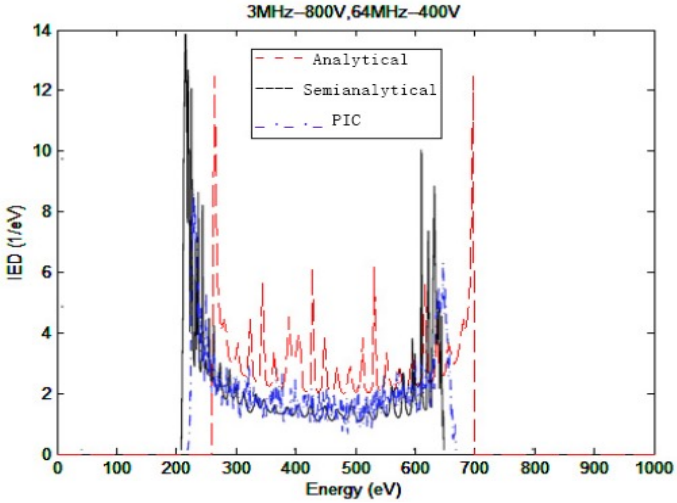

Figure 6.（Color online) Analytical, semianalytical, and PIC IEDs for dual frequency 3MHz - 800V, 64MHz - 400V.

3. PIC Simulations

The simulations are performed using a one-dimensional particle-in-cell code XPDP1. [16] Starting from the initial conditions, particle and field values are sequentially advanced in time. The particle equations of motion are advanced one time step, using fields interpolated from the discrete grid to the continuous particle locations. Next, particle boundary conditions such as absorption are applied. The Monte Carlo collision scheme is applied for electron-neutral collisions. [17] Ion-neutral and neutral-neutral collisions are not considered here. Source terms, charge density ρ, and current density J, for the field equations are accumulated from the continuous particle locations to the discrete mesh locations. The fields are then advanced one time step, and the time step loop starts over again. The cell size Δx, and time step Δt, must be determined from the Debye length λ_D, and the plasma frequency ω_p respectively, for accuracy and stability: $\Delta x < \lambda_D = \sqrt{\varepsilon_0 T_e / en}$ and

$(\Delta t)^{-1} >> \omega_p = \sqrt{e^2 n / \varepsilon_0 m}$. Here, ε_0 is the permittivity of free space, e is the elementary charge, and m is the mass of the lightest species (electrons). A violation of these conditions will result in inaccurate and possibly unstable solutions. After the simulation becomes steady state, the IED is collected over many cycles of the lowest frequency and normalized to unity. The PIC/MCC IED results are then compared with the computational analytical model. In the simulation, the discharge gap is L =0.03 m, consistent with typical processing applications. The gap width is divided into 500 cells, max $\Delta x / \lambda_D \approx 0.8$, and the simulation time step is $\Delta t = 7.63 \times 10^{-12}$, max $\Delta t \omega_p \approx 0.08$, Argon gas is used with p =30 mTorr, *np2c*=1E8, initial density of particles $n_0 = 1 \times 10^{15} \mathrm{m}^{-3}$. These parameters chosen are in order to resolve the Debye length and fulfill simulation stability criteria. The analytical result is shown as the dash line, semi-analytical result as the solid line and the PIC result is shown as the dash-dot line in figures 5, 6. As can be seen, the model predicts the 2 MHz/64 MHz (in figure 5) and the 3 MHz/64 MHz (in figure 6) dual frequency case reasonably well. We have similarly calculated the IEDs for other dual and triple frequency cases and find good agreement. The number of peaks and their energies are reasonably predicted.

4. Conclusions

We have developed the computational analytical model for multi-frequency that result in accurate multi-peaks of the ion energy distributions (IEDs) given the control parameters, which can analytically predict the IEDs multiple peaks and energy width with some plasma parameters provided. This model predicts the IEDs from dual frequencies drives at any voltage, the results are compared with particle-in-cell (PIC) simulations. The IED at a surface is an important parameter for processing in dual radio frequencies driven capacitive discharge. The analytical model is developed for the IED in a low pressure discharge based on a linear transfer function that relates the time-varying sheath voltage to the time-varying ion energy response at the surface. This model is in good agreement with PIC simulations over a wide range of single, dual, and even triple frequency driven capacitive discharge excitations. The present model neglects collisional effects in the sheath, which is the subject of future work.

5. Acknowledgments

The authors gratefully acknowledge the use of PTSG Software from the University of California, Berkeley. This project was supported by the Natural Science Research Project of the Key Laboratory of Guizhou Province Education Bureau Grant No. KY[2014]217, of the Scientific research innovation team in plasma and functional thin film materials of Guizhou Province Education Bureau Grant No.QJTD[2014]38, and of the Key Support Disciplines of Theoretical Physics of Guizhou Province Education Bureau Grant No. ZDXK[2015]38.

6. References

[1] Kawamura E, Vahedi V, Lieberman M A and Birdsall C K, 1999 *Plasma Sources Sci.Technol.* **8**, R45
[2] Benoit-Cattin P and Bernard L –C 1968 *J. Appl. Phys.* **39** 5723
[3] Lieberman M A and Lichtenberg A J 2005 *Principles of Plasma Discharges and Materials Processing*, 2nd ed. Wiley, New York, Chap. 11
[4] Georgieva V, Bogaerts A and Gijbels R 2004 *Phys. Rev. E* **69** 026406
[5] Lee J K, Manuilenko O V, Babaeva N Yu, Kim H C and Shon J W 2005 *Plasma Sources Sci. Technol.* **14** 89
[6] Guan Z Q, Dai Z L and Wang Y N 2005 *Phys. Plasmas* **12** 123502
[7] Wang L H, Dai Z L and Wang Y N 2006 *Chin. Phys. Lett.* **23** 668
[8] Kim H C and Lee J K 2005 *J. Vac. Sci. Technol.* A **23** 651
[9] Olevanov M, Proshina O, Rakhimova T and Voloshin D 2008 *Phys. Rev. E* **78** 026404
[10] Wu A C F, Lieberman M A and Verboncoeur J P 2007 *J. Appl. Phys.* **101** 056105

[11] Rakhimova T V, Braginsky O V, Ivanov V V, Kovalev A S, Lopaev D V, Mankelevich Y A, Olevanov M A, Proshina O V, Rakhimov A T, Vasilieva A N and Voloshin D G 2007 *IEEE Trans. Plasma Sci.* **35** 1229
[12] Lee J K, Manuilenko O V, Babaeva N Y, Kim H C and Shon J W 2005 *Plasma Sources Sci. Technol.* **14** 89
[13] Chen W C, Zhu X M, Zhang S and Pu Y K 2009 *Appl. Phys. Lett.* **94** 211503
[14] Israel D and Riemann K -U 2006 *J. Appl. Phys.* **99** 093303
[15] Wang Y, Lieberman M A，Wu A C F and Verboncoeur J P 2011 *J. Appl. Phys.* **110** 033307
[16] Verboncoeur J P, Alves M V, Vahedi V and Birdsall C K 1993 *J. Comput. Phys.* **104** 321
[17] Vahedi V and Surendra M 1995 *Comput. Phys. Commun.* **87** 179